CORE
Metadata, citation and similar papers at core.ac.uk
Provided by NERC Open Research Archive

NERC Open Research Archive
sharing our research

Centre for Ecology & Hydrology
NATURAL ENVIRONMENT RESEARCH COUNCIL

Article (refereed)

Coyle, Mhairi; Nemitz, Eiko; Storeton-West, Robert; Fowler, David; Cape, J. Neil. 2009 Measurements of ozone deposition to a potato canopy. *Agricultural and Forest Meteorology*, 149 (3-4). 655-666. 10.1016/j.agrformet.2008.10.020

Copyright © 2008 Elsevier B.V.

This version available at http://nora.nerc.ac.uk/6901/

NERC has developed NORA to enable users to access research outputs wholly or partially funded by NERC. Copyright and other rights for material on this site are retained by the authors and/or other rights owners. Users should read the terms and conditions of use of this material at http://nora.nerc.ac.uk/policies.html#access

This document is the author's final manuscript version of the journal article, incorporating any revisions agreed during the peer review process. Some differences between this and the publisher's version remain. You are advised to consult the publisher's version if you wish to cite from this article.

www.elsevier.com

Contact CEH NORA team at
nora@ceh.ac.uk

Measurements of ozone deposition to a potato canopy.

Mhairi Coyle*, Eiko Nemitz, Robert Storeton-West, David Fowler and J Neil Cape
CEH Edinburgh, Bush Estate, Penicuik, Midlothian, EH26 0QB
*+44 (0) 131 445 4343, mcoy@ceh.ac.uk

Abstract

Potatoes are an important staple crop, grown in many parts of the world. Although ozone deposition to many vegetation types has been measured in the field, no data have been reported for potatoes. Such measurements, including the latent heat flux, were made over a fully-grown potato field in central Scotland during the summer of 2006, covering a 4-week period just after rainfall and then dry, sunny weather. The magnitude of the flux was typical of many canopies showing the expected diurnal cycles. Although the bulk-canopy stomatal conductance declined as the field dried out (~300 mmol-O_3 m^{-2} s^{-1} to ~70 mmol-O_3 m^{-2} s^{-1}), the total ozone flux did not follow the same trend, indicating that non-stomatal deposition was significant. Over a dry surface non-stomatal resistance (R_{ns}) was 270-450 s m^{-1}, while over a wet surface R_{ns} was ~50% smaller and both decreased with increasing surface temperature and friction velocity. From the variation with relative humidity (*RH*) it is suggested that three processes occur on leaf surfaces: on a very dry surface ozone is removed by thermal decomposition, possibly enhanced by photolytic reactions in the daytime and so R_{ns} decreases as temperature increases; at 50-70% *RH* a thin film of liquid blocks the "dry" process and resistance increases; above 60-70% *RH* sufficient surface water is present for aqueous reactions to remove ozone and resistance decreases.

Keywords: eddy-correlation; surface conductance; ozone critical levels; AOT40, AFst6; stomatal uptake; non-stomatal; dry deposition

Capsule: Ozone deposition to a potato crop depends not only on stomatal uptake but is enhanced by increasing surface temperature or the presence of water.

Introduction

Tropospheric ozone (O_3) is a secondary pollutant, produced via photochemical reactions of nitrogen oxides (NOx), carbon monoxide (CO) and non-methane volatile organic compounds (VOCs). Although it is a natural constituent of the troposphere, man-made emissions of NOx and VOCs have led to an increase in concentrations (Horowitz, 2006). Average concentrations across much of North America, Europe and Asia are now large enough to cause widespread damage to many types of vegetation, including commercial crops (Ashmore, 2005; Ashmore and Marshall, 1999) and in some regions, peaks of concentration occur that can affect human health (Bell*, et al.*, 2007; Klumpp*, et al.*, 2006). Ozone causes damage to vegetation and humans (as well as other animals) when it is breathed in, through the stomata in the case of plants, and causes a chain of damaging oxidative reactions in internal cells (Larcher, 2001; PORG, 1998).

Many studies of ozone fluxes in the planetary boundary layer (PBL) have been undertaken (e.g. Colbeck and Harrison, 1985; Enders, 1992; Hargreaves*, et al.*, 1992; Stocker*, et al.*, 1987), showing that ozone is always deposited to the Earth' surface, being taken up by plants via stomata as well as being deposited to leaf cuticles and other external surfaces. It has often been assumed that stomatal uptake is the main sink and controlling factor in ozone deposition. However, it has been shown that non-stomatal deposition (to leaf cuticles and soil) can also be significant and varies with surface conditions such as wetness and temperature (Altimir*, et al.*, 2004; Fowler*, et al.*, 2001; Fuentes, 1992; Fuentes*, et al.*, 1992). In addition, over forests, destruction by reaction with biogenic VOCs can provide an additional chemical sink below the flux measurement height (Kurpius and Goldstein, 2003).

Concentration based indices (e.g. Fowler*, et al.*, 1995; Fuhrer*, et al.*, 1997; Legge*, et al.*, 1995) are commonly used to assess the impact of ozone on vegetation, but it is generally accepted that adverse effects are governed by the stomatal flux. The United Nations Economic Commission for Europe (UNECE) recently proposed new critical levels for ozone effects on wheat and potato based on accumulated stomatal uptake (ICP, 2004). These levels were defined using stomatal conductance and ozone exposure data from experiments in controlled environments as there are no measurements of ozone deposition to potatoes in the field. To better understand and model ozone deposition to this crop, field measurements were undertaken during the summer of 2006 in central Scotland. The micrometeorolgical technique of eddy correlation was used to measure the total flux of ozone and water-vapour over a field of potatoes. The water-vapour flux is used to estimate bulk-canopy stomatal conductance which is required to separate the total ozone flux into its stomatal and non-stomatal components. The results are reported here and used to show the importance of non-stomatal deposition in controlling the total flux even when a fully-developed crop is present.

Methods

Fieldsite

The potato field was located at Gilchriston Farm (GT; 55.9°N, 2.8°W, 155 m asl), 24 km south-east of Edinburgh in Central Scotland (Figure 1a). The field was planted with 28.1 ha of *Estima* potatoes surrounded by a border of *Lolium perenne* (1.4 ha, Figure 1b); it is fairly flat but slopes gently down to the south-west. One half of the field was planted with potatoes for seed (13.5 ha) and the other for food (14.6 ha). At the start of measurements on the 9th of July the plants were fully grown at 45 cm tall and flowered two weeks later, in mid-July. On the 3rd of August the crop was de-haulmed; the vegetation is sprayed with a weak acid solution and consequently dies off. The measurements therefore occurred during the period of tuber initiation and development through to harvest.

The instrumentation mast was placed towards the northern edge of the field, about 10 m to the west of the SE to NE centre line (Figure 1b). The fetch (Kormann and Meixner, 2001) varied between *ca.* 250 to 400 m with ~400 m in the prevailing south-westerly wind direction. The topography and planting of the field allowed for measurements in all wind directions.

Micrometeorological theory

Vertical transport between the atmosphere and the surface primarily occurs via turbulent eddies, which are variable in size but are generally smaller towards the surface (Garratt, 1992). The eddies cause high frequency variations in wind speed, air temperature and trace-gas concentration and the eddy-covariance (EC) method is used to analyse these variations and estimate the vertical fluxes of momentum, sensible heat and the trace-gas. The signals can be equated to a mean over time plus the instantaneous departure from the mean, commonly written, following Reynolds averaging as:

$$X = \bar{x} + x' \qquad (1.)$$

where $\bar{x}$ = mean with time, x' = instantaneous deviation from the mean value.

The friction velocity (u_*) which is a measure of momentum transfer to the surface, reflecting the effects of surface roughness and wind velocity, is calculated using:

$$u_* = (-\overline{u'w'})^{0.5}, \qquad (2.)$$

where u and w are the streamwise horizontal and vertical component of wind speed, respectively.

In all conditions the average vertical flux of momentum (τ), or shear stress, is defined as:

$$\tau = -\rho\overline{u'w'} = \rho u_*^2 \qquad (3.)$$

By analogy with this equation the fluxes of sensible heat (H), latent heat (λE) and a trace gas (F_s) can be written as:

$$H = \rho c_p \overline{w'T'} \qquad (4.)$$

$$\lambda E = \lambda \overline{w'q'} \qquad (5.)$$

$$F_s = \overline{w'\chi_s'} \qquad (6.)$$

where ρ = air density (kg m^{-3}), c_p = specific heat at constant pressure for moist air (1.01 J kg^{-1} K^{-1}), T = air temperature (K), λ= latent heat of vaporisation of water (J kg^{-1} K^{-1}, calculated as $\lambda = -2.38\,T+3148.83$), E = water-vapour flux (kg m^{-2} s^{-1}), q = specific humidity of air (mass of water vapour per unit mass of moist air), χ_s = concentration of trace gas *S.*

Hence measurements of the turbulent fluctuations of each component can be used to determine fluxes. This method has the advantage of being quite simple and direct but the turbulent fluctuations occur very rapidly so fast response instruments are required.

The standard resistance analogy (Chamberlain, 1966; Monteith and Unsworth, 1990) where the flux of an entity is equated to a flow of current through a series of resistors, as illustrated in Figure 2, can be used to investigate the influence of surface processes on the atmospheric fluxes. The canopy resistance to ozone deposition, R_c, is found using:

$$R_c = R_t - (R_a + R_{b\_O3}) = \frac{\left|\chi_{O_3}\right|[z-d]}{F_{O_3}[z-d]} - [R_a + R_{b\_O_3}]\,, \qquad (7.)$$

where R_t = total resistance to deposition, z = reference height (2.15 m), d = zero plane displacement height; the height at which canopy effectively becomes closed and all momentum is dissipated (typically 60 to 80% of the canopy height i.e. 0.3 m at Gilchriston), R_a = aerodynamic atmospheric resistance, R_b = sub-laminar boundary layer resistance both found using equations defined by Garland, 1977 and references therein.

For a compound which is only deposited, the inverse of R_t is often considered by micrometeorologists to be the deposition velocity, v_d (m s^{-1}), and was introduced by Chamberlain, 1966 as a useful way of parameterising the deposition process:

$$v_d[z-d] = -F_s[z-d]/\chi[z-d] = -1/R_t \qquad (8.)$$

The reciprocal of a resistance may also be taken to be a conductance (g), by analogy with electrical resistance, and this approach is often taken by plant physiologists who measure the ability of stomata to take in or release gases as a stomatal conductance in mol-gas m^{-2} s^{-1} or m s^{-1}. In the following: R_c is calculated using equation (7) where F_{O3} has been measured by eddy-correlation; resistances are used when discussing ozone deposition to the canopy whereas conductance is used for consideration of stomatal (g_s) responses, although resistance values are given where appropriate for reference.

Instrumentation

The instrumentation consisted of a mast upon which a sonic anemometer (Gill Solent R1012A R2), krypton-hygrometer (Campbell Scientific), fast ozone sensor (CEH Edinburgh, ROFI), pyranometer (Skye Instruments), surface wetness (Campbell Scientific), air temperature and relative humidity sensor (Vaisala HMP45A) were mounted. A laptop and Campbell CR23X data logger were placed in weather proof enclosures within the crop at the base of the mast to log these instruments. Ozone concentrations were measured using a UV-photometric analyser (Thermo 49C) located in a nearby cottage (Figure 1b) and logged on a Campbell 21X datalogger. The additional meteorological variables of rainfall (Cassella tipping bucket) and pressure (Vaisala, PTB101B) were taken from the Bush monitoring site at CEH Edinburgh (BU; 55.9°N, 3.2°W, 180 m asl) 23 km to the west. Soil water content, measured using Campbell TDR probes, at Easter Bush (EB) a grazed field ~300 m from Bush, is also considered.

The Rapid Ozone Flux Instrument (ROFI) used to measure the rapid variations in ozone concentrations and thus calculate the ozone flux using the eddy-covariance method was manufactured at CEH Edinburgh. It follows the same principle as the Gusten instrument (Gusten*, et al.*, 1992) and was designed to match its specification in terms of flow rates and frequency response. Air is rapidly drawn over small disks coated in an ozone sensitive dye and the photons emitted are measured using a photomultiplier tube. The output voltage is proportional to the ozone concentration, but the method is not quantitative and drifts with time, and so the absolute concentration must also be measured using another instrument. Ideally this analyser's inlet would be co-located with the ROFI's but when (as at Gilchriston) this is not possible measurements made nearby are adequate as ozone concentrations vary slowly with distance (Coyle*, et al.*, 2002). The coated disks gradually loose their sensitivity to ozone and so must be replaced approximately every 4 days.

Measured Stomatal and Non-Stomatal Resistance

If transpiration is the only source of water vapour from the surface, i.e. the surface is completely dry and stomata are open, then the bulk-canopy stomatal resistance to water-vapour transfer (R_{s_w}) can be estimated using: canopy surface temperature ($T[z_{0'}]$); vapour pressure at height $d + z_{0'}$, $e[z_{0'}]$; R_a; R_{b_w}; λE and H (Coe*, et al.*, 1995):

$$T[z0'] = T[z\text{-}d] + \frac{H}{\rho c_p}(R_a[z-d] + R_{b\_w}) \qquad (9.);$$

$$e[z0'] = e[z\text{-}d] + \frac{Ep}{\rho\varepsilon}(R_a[z-d] + R_{b\_w}) \ (2); \ R_{s\_w} = \frac{\rho\varepsilon}{p}\frac{e_s[T[z_{0'}]] - e[z_{0'}]}{E}, \qquad (10.)$$

where z = reference height (m), d = zero plane displacement height, $z_{0'}$ = roughness length for dissipation of heat and trace-gases, p = atmospheric pressure (kPa), ε = ratio of the molecular weight of water to that of dry air ≈ 0.62.

Assuming ozone has zero mesophyll resistance (R_{mes}, Omasa*, et al.*, 2002), its stomatal resistance can be calculated by scaling R_{s_w} for molecular diffusivity i.e.:

$R_{s\_w}D_w = R_{s\_O3}D_{O3}$ where D = molecular diffusivity, $D_w/D_{O3} = 1.51$ (Massman, 1998) (11.)

This residual resistance from equation (12) is a combination of R_{ct}, R_{inc} and R_g only as $R_{mes} = 0$, (Figure 2) termed the non-stomatal resistance:

$$R_{ns} = \left(\frac{1}{R_c} - \frac{1}{R_{s\_O3}}\right)^{-1} \qquad (12.)$$

R_{s_o3} and R_{ns} in s m^{-1} can be converted into g_s in mmol m^{-2} s^{-1} using equation 13.

$$g_s = (R_g.T/(p \times 1000)) \times 1000/R \text{ where } R_g = 8.314 \text{ J mol}^{-1} \text{ K}^{-1}. \quad (13.)$$

As the measurements of R_{s_o3} can only be made in dry-daylight conditions the fraction of data suitable for this analysis is greatly reduced (29%).

Data processing and reanalysis

The eddy-correlation data were logged at 20.83 Hz on a laptop to allow the online calculation of fluxes every half hour (using a data acquisition programme written in LabView, National Instruments), while the other variables were logged on Campbell data loggers sampling every 10 seconds and storing 10 minute averages. Standard post-measurement processing procedures were applied to the data. The eddy-correlation measurements were reanalysed using another LabView program which:

- Filtered the time series for large spikes caused by instrument noise.
- Applied the planar fit rotation (Wilczak*, et al.*, 2001) to the sonic anemometer data to correct for any misalignment of the instrument with respect to the mean wind flow direction.
- Corrected the ozone and water-vapour flux for attenuation due to losses at high frequencies, using the method of Horst, 1997.

Further filtering was applied:

- Eddy-correlation methods can only be applied when there is sufficient turbulence, so the *ITC* statistic (integrated turbulence characteristic, Foken*, et al.*, 2004) is used to filter for such conditions (21% of turbulence data were excluded).
- The UV-photometric analyser was calibrated at the start and end of the experiment and as it had not changed, no adjustments to the data were required. As part of the review, these data were compared to measurements at Bush and were found to be very similar (mean GT 26.7, BU 28.2 ppb; maximum GT 83.8, BU 70.0 ppb; minimum GT 3.3, BU 3.9 ppb; σ GT 11.4, BU 9.5 ppb; slope 1.01, $R^2 = 0.70$), confirming the assumption that ozone varies slowly with distance.
- The meteorological measurements were filtered for periods when the instruments may not be functioning correctly, i.e. power failures, site maintenance (15% of turbulence data were excluded).
- Periods where the ROFI output dropped below 30 mV were excluded from the ozone time series as the disk was becoming exhausted.
- The ozone deposition velocity should be less than the maximum possible ($v_{d\_max} = 1/(R_a + R_{b\_O3})$) and so any periods when it exceeded v_{d_max} were excluded from the ozone time series (7% of ozone deposition data were excluded).

- Dry-daylight conditions for the calculation of stomatal resistance were selected using the criteria – no rainfall (as recorded at Bush), $St > 50$ W m^{-2}, dry surface conditions, canopy $RH < 70\%$.

Finally, the time series of each measurement was plotted and visually inspected for inconsistencies. Out of a possible total of 1178 half-hourly values, the percentage data capture of the final data set consists of 99 – 100% basic meteorology, 64% turbulence and λE, 45% ozone flux and 29% stomatal resistance. The preceding filters and reanalysis are applied to account for known theoretical limits to the technique and ensure data quality. This follows the recommended methods for analysing micrometeorological data (Lee*, et al.*, 2004) and the data capture achieved is consistent with other studies.

Results

At the start of July the weather was warm (~15 °C average air temperature) but unsettled with cloud and thundery showers. Between the 7th and the 12th low pressure near Iceland brought unsettled frontal weather with westerly flow and bands of rain separating spells of sunny periods and showers. A large anticyclone developed over Scotland on the 13th and became slow moving to the east for the next two weeks, bringing a long warm, dry spell. Temperatures rose steadily to over 25°C from the 18th, with a peak of 29°C on the 25th, and there were long sunny spells. Eventually, Atlantic fronts crossed the country, bringing rain from the 28th to the 2nd of August, thus the potatoes received no rainfall between the 11th and 28th of July. The local weather and turbulence results reflect these synoptic weather conditions (Figure 3a to d).

Stomatal Conductance

The bulk-canopy stomatal conductance for ozone (derived from the water vapour flux, eqn. (11)) has a mean of 128 mmol-O_3 m^{-2} s^{-1}; summary statistics and the corresponding values calculated as resistances are given in Table 1 while Figure 3e shows a plot of the time series. Other studies have focused on potato's physiological responses to climatic variables and so used direct measurements of conductance on individual leaves. Although there are no similar canopy-level measurements of stomatal conductance for ozone reported in the literature, the magnitude is consistent with the results of Avissar, 1993 who reported values ranging from *ca.* 60 to 600 mmol-O_3 m^2 s^{-1} for individual leaves at different levels in a potato canopy during dry-daytime periods. The plots of g_{s_O3} with canopy temperature ($T_{z0'}$), vapour pressure deficit (*vpd*) and solar radiation (*St*) shown in Figure 4 are also consistent with the results of Gordon*, et al.*, 1997.

At the start of the measurements the plants were well watered due to significant rainfall in early July (Figure 3d). Stomatal conductance averaged ~250 mmol-O_3 m^{-2} s^{-1} and the latent heat flux dominated the surface energy balance (Figure 3c). During the dry spell

g_{s_O3} gradually declined to ~70 mmol-O_3 m^{-2} s^{-1} and latent-heat flux reduced so that sensible heat flux tended to be the larger of the two. Although there are no in-situ soil water content measurements at Gilchriston, the data from the Easter Bush grassland, which is not irrigated, illustrate the likely pattern (Figure 3d) that occurred. As the soil dried out and temperatures increased the plants closed their stomata to reduce water losses by transpiration. It was only after a couple of days of significant rainfall that the vegetation recovered and latent-heat fluxes began to increase (Figures 3c and e).

Ozone deposition to the canopy

As with stomatal conductance there are no other measurements of canopy scale ozone deposition to potato reported in the literature. The mean total flux is -456 ng-O_3 m^{-2} s^{-1} and deposition velocity 6.6 mm s^{-1} (summary statistics are given in Table 1 while the data are plotted in Figure 3f to i) which are similar to fluxes measured over other vegetation (e.g. Fowler, et al., 2001; Padro, 1996; Pio*, et al.*, 2000; Rondon*, et al.*, 1993; Stocker*, et al.*, 1993; Tuovinen*, et al.*, 1998). The hourly median v_d and R_c are plotted in Figure 5a and b respectively and show typical diurnal cycles, with mid-afternoon peaks/troughs respectively (*ibid*; Garland and Derwent, 1979). These diurnal cycles are governed by several processes but mainly: atmospheric turbulence as wind speed and sensible heat flux tend to increase during the day, and so decrease the atmospheric resistance to deposition (Figure 5c); stomatal conductance peaks just before midday (Figure 5d) when conditions are optimal for the plants (large amounts of radiation and low *vpd*). Stomatal conductance was skewed with respect to solar radiation, with larger values during the early morning hours. This is a common observation (e.g. Emberson*, et al.*, 2000) and indicates stomatal closure in the afternoon when the *vpd* increased.

If stomatal uptake is the main factor controlling ozone deposition to a vegetated surface then we would expect to see total deposition decline as stomatal conductance decreases during the monitoring period. However, although it initially decreases, total ozone deposition does not follow the same trend as g_s and peaks during the hot dry period (Figure 3h). It has been suggested that non-stomatal ozone deposition is controlled by surface conditions such as leaf temperature, wetness and solar radiation. For example, Fowler *et al.* (2001) showed that g_{ns} increased with increasing solar radiation over a blanket bog in Central Scotland and hypothesised that this was due to the thermal decomposition of ozone on plant leaf surfaces, while Altimir *et al.* (2004) found that ozone deposition was enhanced to wet needles of Sitka spruce.

Night-time Deposition

If it is assumed that g_s tends towards zero at night then deposition should be mainly non-stomatal at this time (Zhang*, et al.*, 2002). Night-time values of R_c are plotted with friction velocity, surface temperature and relative humidity in Figure 6. As with plots of g_s with environmental variables (Figure 4), there is a lot of scatter in the data, but some trends can be seen; to more clearly detect these, block medians are plotted on the same graphs. As the potato canopy is quite open, it is anticipated that R_{c_night} will decline with increasing friction velocity (or wind speed) as more air penetrates the canopy and increases the surface area available for deposition. This can be seen in Figure 6a, as R_{c_night} clearly declined with increasing u_*. R_{c_night} also varied with *RH* (Figure 6b), increasing slightly as *RH* increased up to 60-70% then decreasing with increasing *RH*. The transition point is similar to that at which hygroscopic-particles tend to dissolve on a leaf cuticle and so enhance its wetability (Burkhardt*, et al.*, 1999), so this may be due to the build up of surface water as *RH* increases: initially, over a very dry surface an increase in humidity forms a thin film of water which occludes sites for ozone deposition on the leaf cuticle and so increases R_c; at ~70% *RH*, the deliquescence of previously deposited particles increases the effective thickness of the water layer so aqueous reactions can occur which increase ozone deposition and so decrease R_c. There was also a tendency for R_{c_night} to decrease with increasing surface temperature, particularly over a dry surface (Figure 6c), supporting the hypothesis that thermal decomposition contributes to non-stomatal deposition.

A cluster of R_{c_night} values of > 1000 s m^{-1} are notable in the plots in Figure 6. They all occur on the night of 16th to 17th July when the canopy resistance increased markedly from 400-500 s m^{-1} to values over 1000 s m^{-1} (Figure 3g), but the reasons for this are not clear. Dew normally forms at night and so we would expect the surface to be wet and so R_c relatively small. The wetness sensor indicates the surface was dry that night but as it does not accurately mimic the thermodynamic properties of the leaves (Klemm*, et al.*, 2002), there may have been some residual moisture present. *RH* was around 60% where it was suggested the deposition process changes from dry-thermal decomposition to aqueous chemistry. Night-time temperatures had been steadily increasing while *RH* declined and so the surface will have been drying out. On the 16th-17th there may only been a thin film of water present that was not sufficient for the aqueous process, but also blocked significant amounts of thermal decomposition occurring on the warm surface. *RH* increased again on subsequent evenings and R_{c_night} decreased to more typical values of ~400 s m^{-1}. It is also possible that the crop was sprayed with a substance that reduced the surface reactivity and so increased R_c, however detailed information on management of the crop is not available; the compounds typically applied to potatoes are pyrethroid or organophosphorus insecticides and NPK fertilizers for which there have been no studies of their surface reactivity with ozone, hence it is not possible to hypothesise further.

Day-time Non-stomatal Deposition

The non-stomatal resistance can also be estimated using Eq. (12) when there are measurements of stomatal conductance during dry-daylight hours (St > 50 W m^{-2}, no rainfall, surface dry and RH < 70%). These values are plotted against the relevant variables in Figure 7: as with $R_{\mathrm{c\_night}}$ there is a lot of scatter in the data but some trends can be detected:

- R_{ns} tended to decline with increasing u_*; as with R_{c_night} this was due to an increase in the surface area available for deposition as more air penetrates the canopy and may also come into contact with the soil (Figure 7a).
- R_{ns} declined with increasing solar radiation, from ~300 s m^{-1} below 200 W m^{-2} to ~150 s m^{-1} above 200 W m^{-2} (Figure 7b); as surface temperature is directly related to St this may be due to the proposed thermal decomposition process although additional ozone photolysis on the surface may play a part. Emissions of reactive volatile organic compounds (VOCs) from potatoes have been reported to be negligible (Drewitt*, et al.*, 1998) so VOC/ozone reactions are unlikely to be significant. These results are very similar to the results obtained by Fowler, et al., 2001), following an essentially identical response curve (Figure 7e).
- The data are very scattered below ~25°C but there is an indication that R_{ns} declined with increasing $T_{z0'}$. It was found that there was a transition in surface responses at about 60-70% RH for the night-time data so to exclude these conditions the data was filtered to remove measurements where RH > 60%. This reduced the scatter in the R_{ns}-$T_{z0'}$ response, showing a clearer decrease in R_{ns} with increasing $T_{z0'}$ (Figure 7c).
- There are limited data of R_{ns} for RH < 70%, but a clear decline in R_{ns} with RH can be seen above 50%; below 50% the data are more scattered, but except for the first data point an increase in R_{ns} with RH is evident (Figure 7d). The first data point is the median of measurements taken over the 16th of July when particularly large night-time canopy resistances were measured (the fourth data point is mainly from this period as well).

Critical Levels and Stomatal Uptake

As part of the UNECE Convention on Long Range Transboundary Air Pollution (CLRTAP) several expert groups, known as International Cooperative Programmes (ICP) have been set up to examine relevant areas of science. One of these is the ICP-Vegetation which investigates the impacts of air pollutants on crops and (semi-) natural vegetation. The uptake based critical level for ozone effects on potato has been set at an *AFst6* of 5 mmol m^{-2} PLA (Projected Leaf Area) by ICP-Vegetation (ICP, 2004) where AFst6 is the accumulated stomatal uptake over 6 nmol m^{-2} s^{-1} during daylight hours for either 1130°C-days or 70 days starting at plant emergence. The site was not monitored from sowing of the crop but using a temperature based phenological model (*ibid*) the accumulation period was estimated to be from the 8th of May to the 25th of July (78 days from emergence). Measurements were not made for all of this period but to exceed the critical level this would require the crop to take up, at least, 68 nmol m^{-2} PLA per day on average. The maximum daily accumulation measured during the experiment was only 35 nmol m^{-2} PLA so it is highly unlikely that this crop suffered any adverse affects from ozone exposure, according to the flux based approach. However, the AOT40 critical level (accumulated concentration over 40 ppb during daylight hours) for the growing season of an agricultural crop is set at 3000 ppb h^{-1} and this was exceeded during the measurement period, with an AOT40 of 3942 ppb h^{-1}. Therefore an assessment based on AOT40 would have predicted some damage to the crop.

Summary and Conclusions

A comprehensive dataset of meteorological variables, ozone and water-vapour fluxes measured over a potato crop have been presented. The measurements show that significant amounts of ozone are deposited to the surface even when the vegetation is not very active. This shows that non-stomatal sinks are an important pathway for ozone deposition which can equal or exceed stomatal uptake in certain conditions (Figure 8). The non-stomatal sink also varies with surface conditions rather than simply scaling with *LAI*, as is often assumed.

Using the night-time data only, it was shown that R_{c_night} is dependent on surface wetness and temperature as well as friction velocity. The dependence on friction velocity is simply due to more air penetrating the canopy as wind speeds increase, and so increasing the surface area available for deposition. Overall R_{c_night} tends to be smaller when the surface is wet (median 211 sm^{-1}) compared with dry (median of 453 s m^{-1}) which is contrary to the common assumption the ozone deposition rates to wet vegetation are small due to ozone's poor solubility (e.g. Erisman*, et al.*, 1994). However other studies have shown that some canopies exhibit higher deposition rates when wet, for example Altimir, et al., 2004; Fuentes*, et al.*, 1994; Grantz*, et al.*, 1995; Pleijel*, et al.*, 1995; Zhang, et al., 2002. The data indicate three main regimes and possible processes: ozone deposition increasing as the temperature increases on a dry surface due to thermal decomposition; decreased deposition on surfaces with a thin film of water present as thermal decomposition is blocked, when *RH* ≤60%; enhanced deposition on a fully wetted surface as sufficient water is present for aqueous chemistry to occur, *RH* > 70%. Studies of ozone deposition to seawater have shown that the presence of dissolved surfactants can increase deposition rates (Chang*, et al.*, 2004; McKay*, et al.*, 1992) and it is likely that many potentially reactive compounds are present in surface water on vegetation. For example ozone can act as an oxidising agent for SO_2 in water and if sufficient NH_3 is also present to increase the pH, this could represent a significant sink for O_3 (Flechard*, et al.*, 1999).

The dry-daytime non-stomatal resistance, R_{ns}, was also examined in isolation and found to exhibit the same relationship with temperature and also to decrease as solar radiation increased. As solar radiation and temperature are closely coupled this may simply be due to thermal processes. However, it is possible that other photolytic reactions occur as the median R_{ns} for a dry surface is lower (median 267 s m^{-1}) than that for a dry night-time canopy (median 453 s m^{-1}). The relationship of R_{ns} to *St* is virtually identical to that observed by Fowler, et al., 2001 for a moorland canopy indicating that similar processes are occurring at both sites.

The measurements of R_{ns} are restricted to dry periods, for which R_s could be estimated, hence, fully wetted surfaces cannot be examined. However, the relationship of R_{ns} with *RH* is similar to that seen for R_{c_night} indicating that the day-time processes are similar, although the transition point may occur at slightly lower relative humidity (50-60%).

These processes may be occurring on both the external parts of the plants and the soil surface beneath the plant as studies have shown soil deposition rates can depend on soil moisture and chemistry (Chang*, et al.*, 2002; Sorimachi and Sakamoto, 2007; Wesely*, et al.*, 1981). However as the surface area of vegetation greatly exceeds the soil area and its density inhibits turbulent transfer to the soil, is assumed that most of the deposition occurs on the upper parts of the plants. To more clearly understand the processes involved in ozone deposition to leaf cuticles or soil alone, controlled chamber studies are required. These will allow variables such as surface chemistry, humidity, temperature and radiation to be independently examined. Some initial experiments of this type have been undertaken (Hamilton*, et al.*, 2007) and indicated that surface temperature was indeed a controlling variable: ozone deposition increased with temperature on stainless steel, aluminium foil and wax surfaces.

At present, many models use the formula of Wesely, 1989 where:

$$R_{ns} = R_{ext}/SAI,\ SAI = \text{surface area index} \approx LAI, \text{ for ozone } R_{ext} = 2500 \text{ s m}^{-1} \qquad (14.)$$

giving a R_{ns} of 833 s m^{-1} for a typical potato crop with *LAI* ~3 m^{-2} m^{-2}. This is significantly greater than the median value observed in this study of only 170 s m^{-1}, although the results do vary greatly with a standard deviation of 724 s m^{-1}. Zhang, et al., 2002 proposed a new model for R_{ns} based on an analysis of night-time resistances for a range of vegetation types (mixed forest, deciduous forest, corn, soy bean and pasture). Although temperature was not considered as a controlling variable their results are similar to those found here in that R_{ns} was smaller by ~50% for wet compared to dry surfaces and it declined with u_* and *RH*. Applying this model to our data gave better estimates than using a simple *SAI* formula in that it correlated with the measured R_{c_night}

for some periods but still overestimated R_{c_night} for much of time, giving median values of 904 and 573 s m^{-1} for wet and dry surfaces, respectively.

A change in model parameterisation is not suggested here as measurements from a wider range of sites and conditions should be used but these results show that such an exercise should be undertaken. To fully examine and parameterise surface processes, measurements or models of stomatal conductance need to be included to allow day-night differences to be assessed. Although there are few measurements for potatoes there are many other datasets for different vegetation types that could be utilised.

The measurements do not imply damage based on the AFst6 critical level, despite the fact that the AOT40 limit value is exceeded. This finding highlights the inconsistency caused by using an atmospheric concentration based approach as although ozone concentrations may be large, stomatal uptake which causes the damage may be small. This is particularly evident during warm-dry conditions which favour ozone production but reduce stomatal opening, as occurred during these measurements, even at a NW European site located in a climate where drought is not normally considered to be a limitation to stomatal functioning.

Acknowledgements

We are very grateful to: Mr Keith Maxwell of Gilchriston Farm for allowing us to use his field and providing access to mains electricity; the contractors, Crop Chemicals (Drem, East Lothian, Scotland), for letting us know when the dehaulming would occur and giving us time to remove the equipment; CEH for funding the work from the institute's budget and Defra for providing funding from project 1/3/201 (Ozone Umbrella: Effects of Ground-level Ozone on (Upland) Vegetation in the UK).

References

Altimir, N., Tuovinen, J. P., Vesala, T., Kulmala, M. and Hari, P., (2004): Measurements of ozone removal by Scots pine shoots: calibration of a stomatal uptake model including the non-stomatal component, *Atmospheric Environment*, 38, 2387-2398

Ashmore, M. R., (2005): Assessing the future global impacts of ozone on vegetation, *Plant, Cell and Environment*, 28, 949-964

Ashmore, M. R. and Marshall, F. M., (1999): Ozone impacts on agriculture: An issue of global concern, Advances in Botanical Research Incorporating Advances in Plant Pathology, Vol 29, 31-52, *Academic Press*

Avissar, R., (1993): Observations of Leaf Stomatal Conductance at the Canopy Scale - an Atmospheric Modeling Perspective, *Boundary-Layer Meteorology*, 64, 127-148

Bell, M. L., Goldberg, R., Hogrefe, C., Kinney, P. L., Knowlton, K., Lynn, B., Rosenthal, J., Rosenzweig, C. and Patz, J. A., (2007): Climate change, ambient ozone, and health in 50 US cities, *Climatic Change*, 82, 61-76

Burkhardt, J., Kaiser, H., Goldbach, H. and Kappen, L., (1999): Measurements of electrical leaf surface conductance reveal recondensation of transpired water vapour on leaf surfaces, *Plant Cell and Environment*, 22, 189-196

Chamberlain, A. C., (1966): Transport of gases to and from grass and grass-like surfaces, *Proceedings of the Royal Society of London A*, 290, 236-260

Chang, H. M., Chang, L. F. W. and Jeng, F. T., (2002): Interfacial transfer velocities of ozone dry deposition over agricultural soils: Experimental and theoretical analysis, *Journal of Environmental Science and Health Part B Pesticides Food Contaminants and Agricultural Wastes*, 37, 507-518

Chang, W., Heikes, B. G. and Lee, M., (2004): Ozone deposition to the sea surface: chemical enhancement and wind speed dependence, *Atmospheric Environment*, 38, 1053-1059

Coe, H., Gallagher, M. W., Choularton, T. W. and Dore, C., (1995): Canopy scale measurements of stomatal and cuticular o3 uptake by sitka spruce, *Atmospheric Environment*, 29, 1413-1423

Colbeck, I. and Harrison, R. M., (1985): Dry deposition of ozone: some measurements ofdeposition velocity and of vertical profiles to 100 metres, *Atmospheric Environment (1967)*, 19, 1807-1818

Coyle, M., Smith, R. I., Stedman, J. R., Weston, K. J. and Fowler, D., (2002): Quantifying the spatial distribution of surface ozone concentration in the UK, *Atmospheric Environment*, 36, 1013-1024

Drewitt, G. B., Curren, K., Steyn, D. G., Gillespie, T. J. and Niki, H., (1998): Measurement of biogenic hydrocarbon emissions from vegetation in the lower fraser valley, British Columbia, *Atmospheric Environment*, 32, 3457-3466

Emberson, L. D., Ashmore, M. R., Cambridge, H. M., Simpson, D. and Tuovinen, J. P., (2000): Modelling stomatal ozone flux across Europe, *Environmental Pollution*, 109, 403-413

Enders, G., (1992): Deposition of Ozone to a Mature Spruce Forest - Measurements and Comparison to Models, *Environmental Pollution*, 75, 61-67

Erisman, J. W., Vanpul, A. and Wyers, P., (1994): Parametrization of Surface-Resistance for the Quantification of Atmospheric Deposition of Acidifying Pollutants and Ozone, *Atmospheric Environment*, 28, 2595-2607

Flechard, C. R., Fowler, D., Sutton, M. A. and Cape, J. N., (1999): A dynamic chemical model of bi-directional ammonia exchange between semi-natural vegetation and the atmosphere, *Quarterly Journal of the Royal Meteorological Society*, 125, 2611-2641

Foken, T., Gockede, M., Mauder, M., Mahrt, L., Amiro, B. and Munger, W., (2004): Post-field data quality control, Handbook of Micrometeorology, 181-208, *Kluwer*

Fowler, D., Flechard, C., Cape, J. N., Storeton-West, R. L. and Coyle, M., (2001): Measurements of ozone deposition to vegetation quantifying the flux, the stomatal and non-stomatal components, *Water Air and Soil Pollution*, 130, 63-74

Fowler, D., Smith, R. I., Coyle, M., Weston, K. J., Davies, T. D., Ashmore, M. R. and Brown, M., (1995): Quantifying the fine scale (1kmx1km) exposure and effects of ozone .1. Methodology and application for effects on forests, *Water, Air, and Soil Pollution*, 85, 1479-1484

Fuentes, J. D., (1992): Effect of foliage surface wetness on the deposition of ozone, *The University of Geulph*,

Fuentes, J. D., Gillespie, T. J. and Bunce, N. J., (1994): Effects of Foliage Wetness on the Dry Deposition of Ozone onto Red Maple and Poplar Leaves, *Water Air and Soil Pollution*, 74, 189-210

Fuentes, J. D., Gillespie, T. J., Denhartog, G. and Neumann, H. H., (1992): Ozone Deposition onto a Deciduous Forest During Dry and Wet Conditions, *Agricultural and Forest Meteorology*, 62, 1-18

Fuhrer, J., Skarby, L. and Ashmore, M. R., (1997): Critical levels for ozone effects on vegetation in Europe, *Environmental Pollution*, 97, 91-106

Garland, J. A., (1977): The dry deposition of sulphur dioxide to land and water surfaces., *Proceedings of the Royal Society of London A*, 354, 245-268

Garland, J. A. and Derwent, R. G., (1979): Destruction at the ground and the diurnal cycle of concentration of ozone and other gases, *Quarterly Journal Royal Meteorological Society*, 105, 169-183

Garratt, J. R., (1992): The atmospheric boundary layer., Cambridge atmospheric and space science, *Cambridge University Press*

Gordon, R. J., Brown, D. M. and Dixon, M. A., (1997): Stomatal resistance of three potato cultivars as influenced by soil water status, humidity and irradiance, *Potato Research*, 40, 47-57

Grantz, D. A., Zhang, X. J., Massman, W. J., Denhartog, G., Neumann, H. H. and Pederson, J. R., (1995): Effects of stomatal conductance and surface wetness on ozone deposition in field-grown grape, *Atmospheric Environment*, 29, 3189-3198

Gusten, H., Heinrich, G., Schmidt, R. W. H. and Schurath, U., (1992): A Novel Ozone Sensor for Direct Eddy Flux Measurements, *Journal of Atmospheric Chemistry*, 14, 73-84

Hamilton, R., Cape, J. N. and Heal, M. R., (2007): Reactions of ozone at plant surfaces, Second ACCENT Symposium: ATMOSPHERIC COMPOSITION CHANGE: CAUSES AND CONSEQUENCES, Local to Global, Urbino, Italy

Hargreaves, K. J., Fowler, D., Storetonwest, R. L. and Duyzer, J. H., (1992): The Exchange of Nitric-Oxide, Nitrogen-Dioxide and Ozone between Pasture and the Atmosphere, *Environmental Pollution*, 75, 53-59

Horowitz, L. W., (2006): Past, present, and future concentrations of tropospheric ozone and aerosols: Methodology, ozone evaluation, and sensitivity to aerosol wet removal, *Journal of Geophysical Research-Atmospheres*, 111,

Horst, T. W., (1997): A simple formula for attenuation of eddy fluxes measured with first-order-response scalar sensors, *Boundary-Layer Meteorology*, 82, 219-233

ICP, (2004): Mapping Manual 2004, *UNECE-LRTAP*, http://www.icpmapping.org

Klemm, O., Milford, C., Sutton, M. A., Spindler, G. and van Putten, E., (2002): A climatology of leaf surface wetness, *Theoretical and Applied Climatology*, 71, 107-117

Klumpp, A., Ansel, W., Klumpp, G., Calatayud, V., Garrec, J. P., He, S., Penuelas, J., Ribas, A., Ro-Poulsen, H., Rasmussen, S., Sanz, M. J. and Vergne, P., (2006): Ozone pollution and ozone biomonitoring in European cities. Part I: Ozone concentrations and cumulative exposure indices at urban and suburban sites, *Atmospheric Environment*, 40, 7963-7974

Kormann, R. and Meixner, F. X., (2001): An analytical footprint model for non-neutral stratification, *Boundary-Layer Meteorology*, 99, 207-224

Kurpius, M. R. and Goldstein, A. H., (2003): Gas-phase chemistry dominates O-3 loss to a forest, implying a source of aerosols and hydroxyl radicals to the atmosphere - art. no. 1371, *Geophysical Research Letters*, 30, 1371

Larcher, W., (2001): Physiological Plant Ecology, *Springer-Verlag*

Lee, X., Massman, W. J. and Law, B., (2004): Handbook of Micrometeorology: A guide for surface flux measurement and analysis, Handbook of Micrometeorology, *Kluwer*

Legge, A. H., Grunhage, L., Nosal, M., Jager, H. J. and Krupa, S. V., (1995): Ambient ozone and adverse crop response: An evaluation of North American and European data as they relate to exposure indices and critical levels, *Journal of Applied Botany-Angewandte Botanik*, 69, 192-205

Massman, W. J., (1998): A review of the molecular diffusivities of H2O, CO2, CH4, CO, O-3, SO2, NH3, N2O, NO, AND NO2 in air, O-2 AND N-2 near STP, *Atmospheric Environment*, 32, 1111-1127

McKay, W. A., Stephens, B. A. and Dollard, G. J., (1992): Laboratory measurements of ozone deposition to sea-water and other saline solutions, *Atmospheric Environment Part A-General Topics*, 26, 3105-3110

Monteith, J. L. and Unsworth, M., (1990): Principles of Environmental Physics, *Edward Arnold*

Omasa, K., Endo, R., Tobe, K. and Kondo, T., (2002): Gas diffusion model analysis of foliar absorption of organic and inorganic air pollutants, *Phyton-Annales Rei Botanicae*, 42, 135-148

Padro, J., (1996): Summary of ozone dry deposition velocity measurements and model estimates over vineyard, cotton, grass and deciduous forest in summer, *Atmospheric Environment*, 30, 2363-2369

Pio, C. A., Feliciano, M. S., Vermeulen, A. T. and Sousa, E. C., (2000): Seasonal variability of ozone dry deposition under southern European climate conditions, in Portugal, *Atmospheric Environment*, 34, 195-205

Pleijel, H., Karlsson, G. P., Danielsson, H. and Sellden, G., (1995): Surface wetness enhances ozone deposition to a pasture canopy, *Atmospheric Environment*, 29, 3391-3393

PORG, (1998): Ozone in the United Kingdom, Fourth Report of the Photochemical Oxidants Review Group, *The Department of the Environment Transport and the Regions*, http://www.nbu.ac.uk/pollution/docs/PORGiv.htm

Rondon, A., Johansson, C. and Granat, L., (1993): Dry Deposition of Nitrogen-Dioxide and Ozone to Coniferous Forests, *Journal of Geophysical Research-Atmospheres*, 98, 5159-5172

Sorimachi, A. and Sakamoto, K., (2007): Laboratory Measurement of Dry Deposition of Ozone onto Northern Chinese Soil Samples, *Water, Air, & Soil Pollution: Focus*, 7, 181-186

Stocker, D. W., Burkhardt, M. R. and Stedman, D. H., (1987): The Flux and Deposition Velocities of Nitrogen-Dioxide and Ozone to Desert Soil by Eddy-Correlation, *Abstracts of Papers of the American Chemical Society*, 193, 175-ENVR

Stocker, D. W., Stedman, D. H., Zeller, K. F., Massman, W. J. and Fox, D. G., (1993): Fluxes of nitrogen-oxides and ozone measured by eddy-correlation over a shortgrass prairie, *Journal of Geophysical Research-Atmospheres*, 98, 12619-12630

Tuovinen, J. P., Aurela, M. and Laurila, T., (1998): Resistances to ozone deposition to a flark fen in the northern aapa mire zone, *Journal of Geophysical Research-Atmospheres*, 103, 16953-16966

Wesely, M. L., (1989): Parameterization of Surface Resistances to Gaseous Dry Deposition in Regional-Scale Numerical-Models, *Atmospheric Environment*, 23, 1293-1304

Wesely, M. L., Cook, D. R. and Williams, R. M., (1981): Field Measurement of Small Ozone Fluxes to Snow, Wet Bare Soil, and Lake Water, *Boundary-Layer Meteorology*, 20, 459-471

Wilczak, J. M., Oncley, S. P. and Stage, S. A., (2001): Sonic Anemometer Tilt Correction Algorithms, *Boundary-Layer Meteorology*, 99, 127-150

Zhang, L. M., Brook, J. R. and Vet, R., (2002): On ozone dry deposition - with emphasis on non-stomatal uptake and wet canopies, *Atmospheric Environment*, 36, 4787-4799

Table 1 Data summary (SE = $\sigma/(n-1)^{-2}$, n = number of data points)

		Mean	Median	Max	Min	σ	SE
g_{s_O3}	mmol m^{-2} s^{-1}	128	109	401	22	72.6	3.9
R_{s_O3}	s m^{-1}	429	372	1822	105	249.4	13.5
v_{d_o3}	mm s^{-1}	6.6	5.7	23.7	0.4	4.26	0.17
	night-time*	3.9	3.2	10.9	0.4	2.56	0.20
R_{c_O3}	s m^{-1}	194	109	2361	6	280.8	11.3
	night-time	343	204	2361	13	424.1	33.3
	Dry night	693	453	2361	80	654.4	107.6
	Wet night	262	211	1107	13	225.0	31.2
R_{ns}	s m^{-1}	333	170	8907	1	723.6	44.0
	$RH \leq 50\%$	413	267	6111	3	691.7	42.2
F_{O3}	ng m^{-2} s^{-1}	-456	-380	-2340	-8	336.9	13.6
	night-time	-221	-181	-1047	-8	166.8	13.1
χ_{O3}(1 m)	μg m^{-3}	47.1	42.9	159.7	2.8	24.04	0.97
	night-time	43.4	41.0	159.7	2.8	21.30	1.64
R_a(1 m)	s m^{-1}	38	27	219	1	31.0	1.1
R_{b_O3}	s m^{-1}	34	25	421	13	33.2	1.1

* Night-time is defined as half-hours when the solar zenith angle is greater than 85° and solar radiation is less than 20 W m^{-2}

List of tables and figures

Table 1 Data summary (SE = $\sigma /(n-1)^{-2}$, n = number of data points)

Figure 1 a. Location of Gilchriston Farm in Central Scotland (55.9°N, 2.8°W, 155 m asl), b. sketch of the fieldsite showing the location of the mast and other equipment.

Figure 2 The deposition resistance analogy for ozone deposition, showing the main components controlling the rate of surface deposition.

Figure 3 Summary of half-hourly average ozone flux and other measurements: a total solar radiation (S_t) and ambient air temperature (T_a); b windspeed at 1 m ($U(1m)$) and friction velocity (u_*); c sensible (H) and latent-heat (λE) fluxes; d soil water content (SWC) and daily total rainfall measured at Easter Bush and Bush respectively; e vapour pressure deficit (*vpd*) and stomatal conductance (g_{s_O3}); f ozone deposition velocity (v_d); g total canopy resistance to ozone (R_{cO3}); h ozone flux (F_{O3}); i ozone concentration (χ_{O3}, nmol mol^{-1} = ppb).

Figure 4 The total bulk canopy conductance for ozone uptake (g_{s_O3}) against surface temperature ($T_{z0'}$), vapour pressure deficit (*vpd*) and total solar radiation (S_t).

Figure 5 Hourly median diurnal cycles in: a ozone deposition velocity; b, total canopy resistance to ozone deposition; c, aerodynamic and sub-laminar boundary layer resistance to ozone; d, bulk-canopy stomatal conductance for ozone uptake, vapour pressure deficit and total solar radiation (average).

Figure 6 Half-hourly measurements of night-time total canopy resistance to ozone against (a) friction velocity, (b) relative humidity and (c) surface temperature. Squares are points when the surface was completely wet, diamonds are very dry while circles are block medians of all data points (black where the standard error is <50%), error bars are ± one standard error. The ranges used for the block medians are u_* 0.025 m s^{-1}, *RH* 2.5%, $T_{z0'}$ 1°C.

Figure 7 Half hourly estimates and block medians of non-stomatal resistance to ozone for dry-daylight conditions against: a friction velocity, 0.1 m s^{-1} median; b total solar radiation, 50 W m^{-2} median; c surface temperature for all data and excluding $RH \geq 60\%$, 1 °C median; d relative humidity, 2% median; e R_{ns} estimates from Auchencorth Moss (20 W m^{-2}) and non-linear regression curves for those data and Gilchriston Farm. Error bars are ± one standard error.

Figure 8 The percentage of the total flux that is either stomatal or non-stomatal.

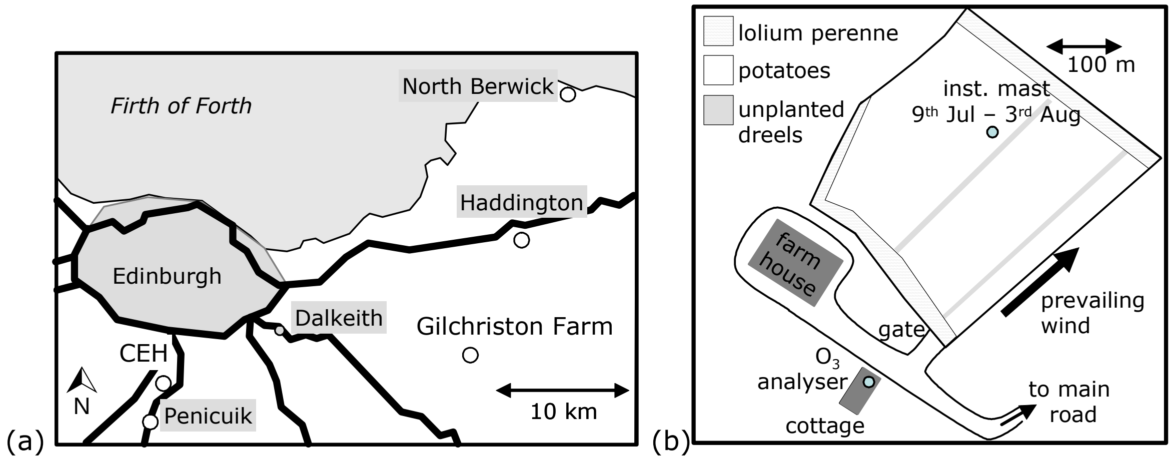

Figure 1 (a). Location of Gilchriston Farm in Central Scotland (55.9°N, 2.8°W, 155 m asl), (b). sketch of the fieldsite showing the location of the mast and other equipment.

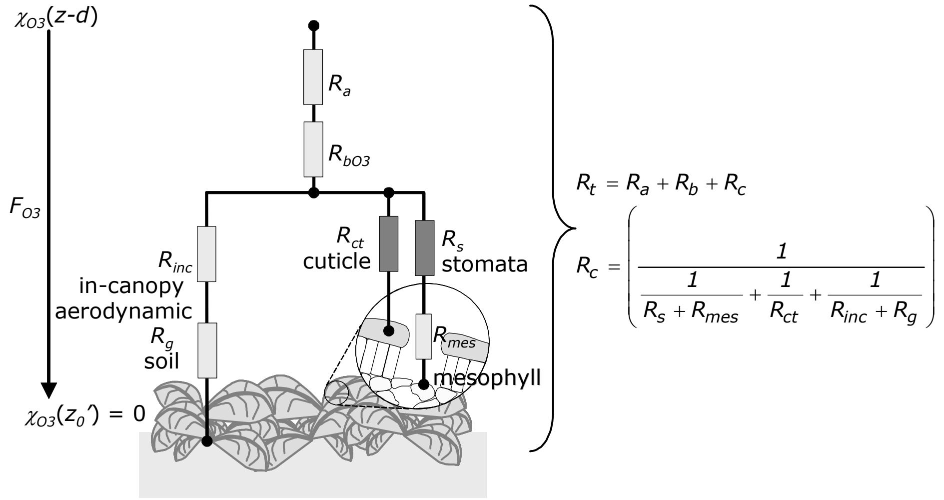

Figure 2 The deposition resistance analogy for ozone deposition, showing the main components controlling the rate of surface deposition.

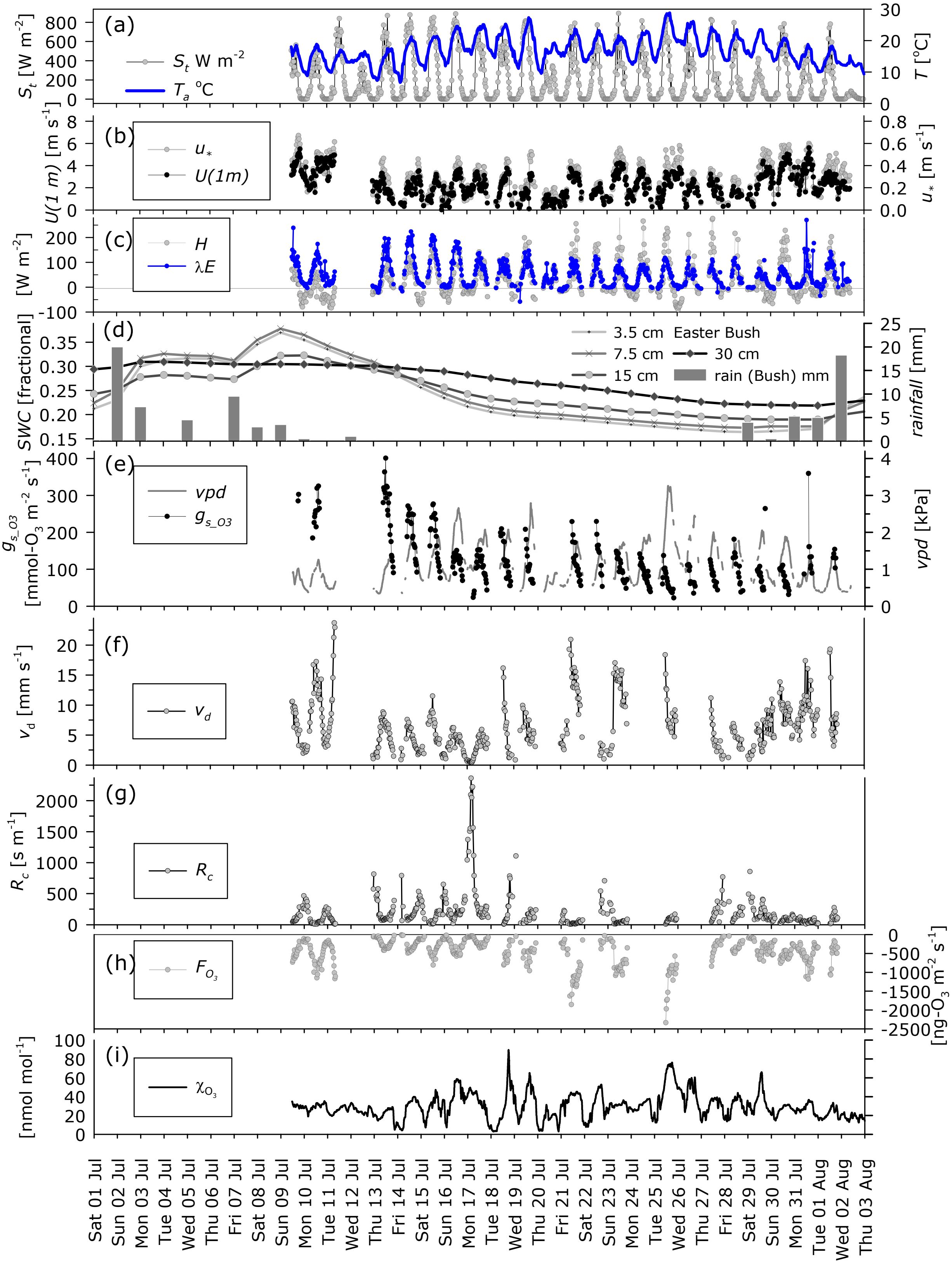

Figure 3 Summary of half-hourly average ozone flux and other measurements: a total solar radiation (S_t) and ambient air temperature (T_a); b windspeed at 1 m ($U(1m)$) and friction velocity (u_*); c sensible (H) and latent-heat (λE) fluxes; d soil water content (SWC) and daily total rainfall measured at Easter Bush and Bush respectively; e vapour pressure deficit (vpd) and stomatal conductance (g_{s_O3}); f ozone deposition velocity (v_d); g total canopy resistance to ozone (R_{cO3}); h ozone flux (F_{O3}); i ozone concentration (χ_{O3}, nmol mol^{-1} = ppb).

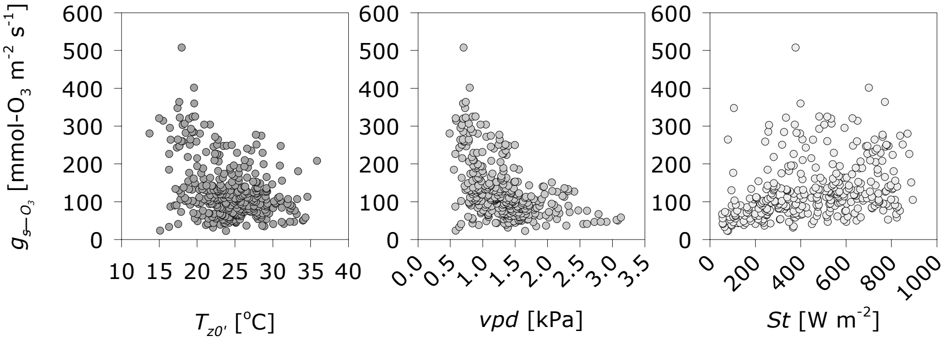

Figure 4. The total bulk canopy conductance for ozone uptake (g_{s_O3}) against surface temperature ($T_{z0'}$), water vapour pressure deficit (*vpd*) and total solar radiation (S_t).

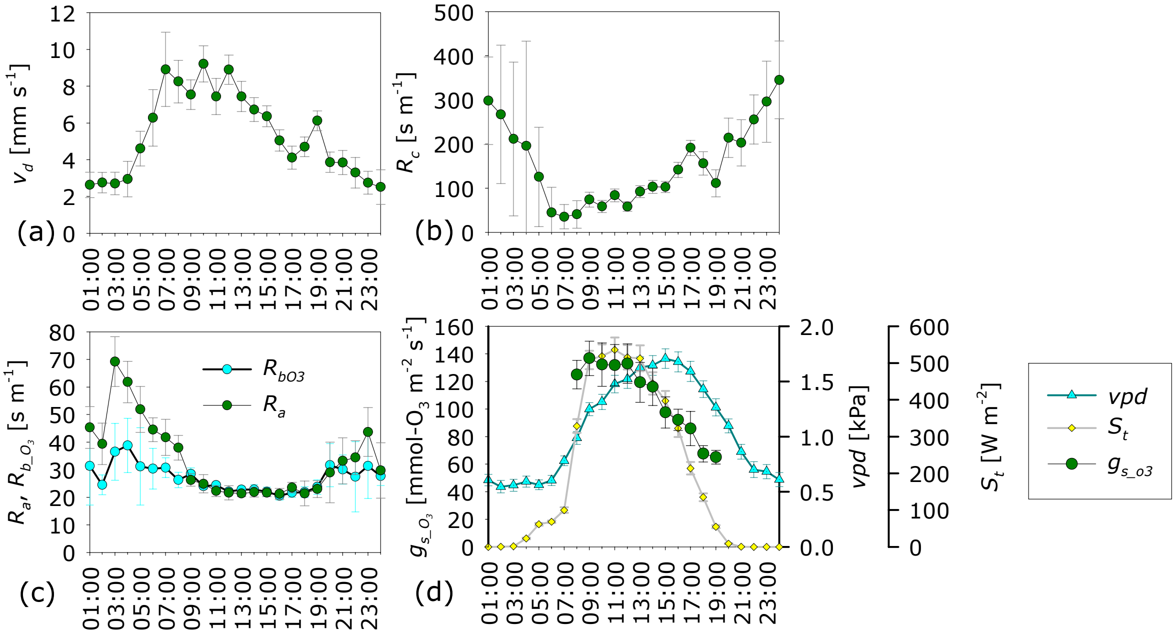

Figure 5 Hourly median diurnal cycles in: (a) ozone deposition velocity; (b) total canopy resistance to ozone deposition; (c) aerodynamic (R_a) and sub-laminar boundary layer resistance (R_{bO3}) to ozone; (d) bulk-canopy stomatal conductance for ozone uptake, vapour pressure deficit and total solar radiation (average), error bars are ± one standard error.

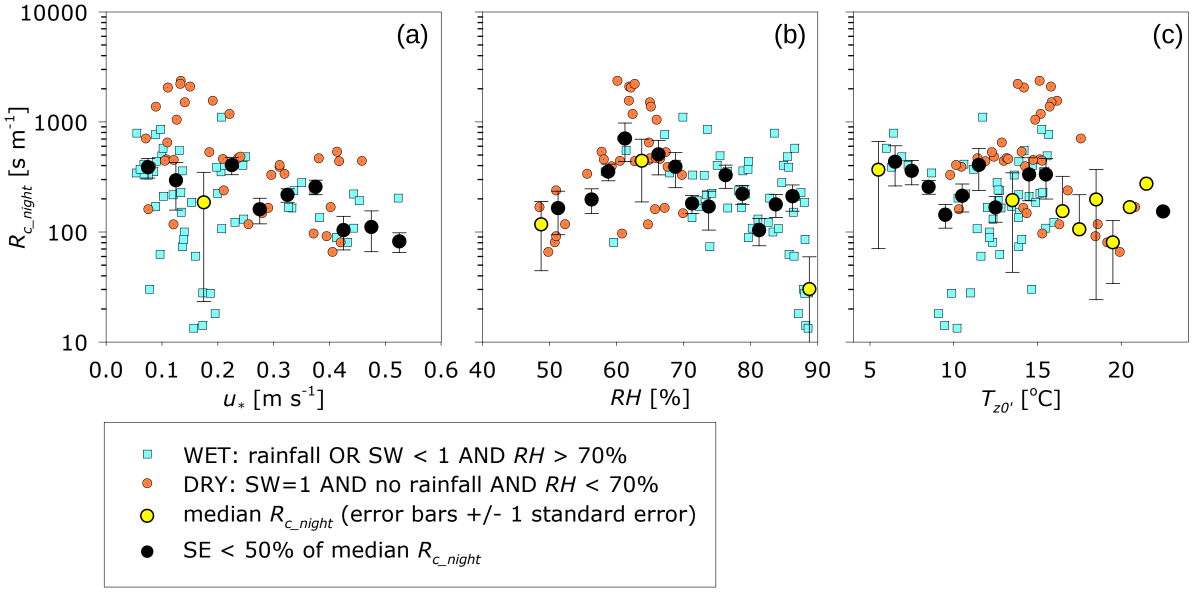

Figure 6 Half-hourly measurements of night-time total canopy resistance to ozone against (a) friction velocity, (b) relative humidity and (c) surface temperature. Squares are points when the surface was completely wet, diamonds are very dry while circles are block medians of all data points (black where the standard error is <50%), error bars are ± one standard error. The ranges used for the block medians are u_* 0.025 m s^{-1}, RH 2.5%, $T_{z0'}$ 1°C.

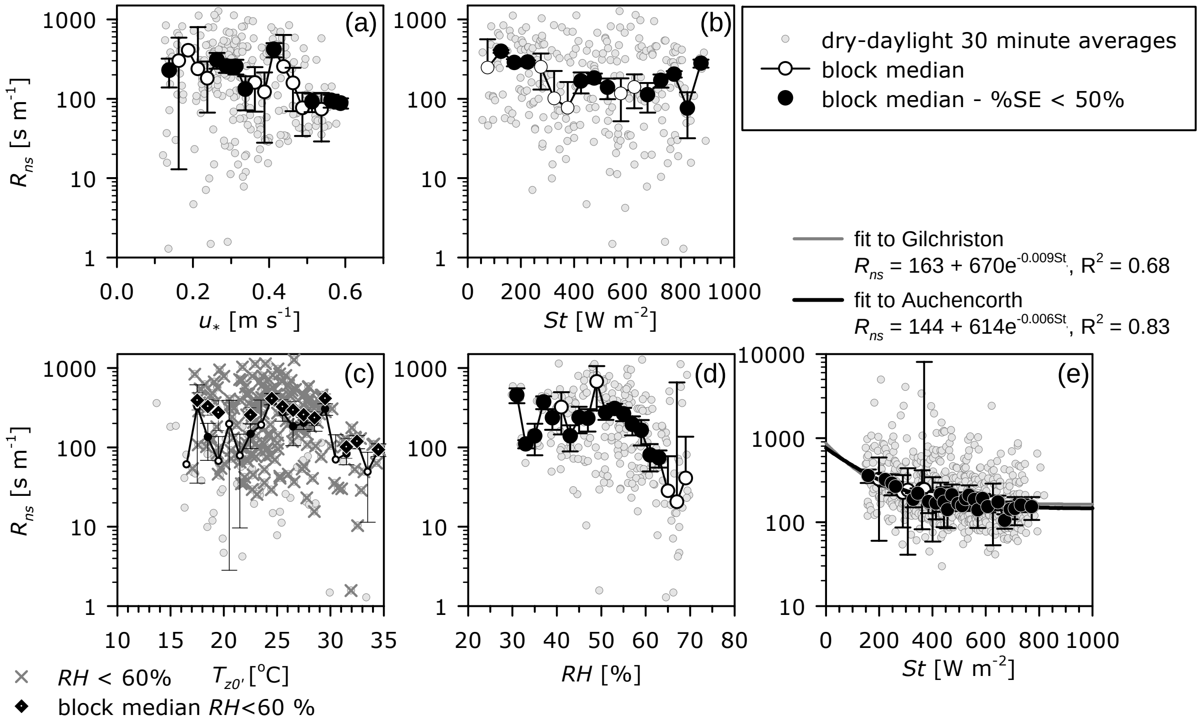

Figure 7. Half hourly estimates and block medians of non-stomatal resistance to ozone for dry-daylight conditions against: (a) friction velocity, 0.1 m s^{-1} bins; (b) total solar radiation, 50 W m^{-2} bins; (c) surface temperature for all data and excluding $RH \geq 60\%$, 1 °C bins; (d) relative humidity, 2% bins; (e) R_{ns} estimates from Fowler *et al.* (2001) (20 W m^{-2}) and non-linear regression curves for those data and Gilchriston Farm. Error bars are ± one standard error.

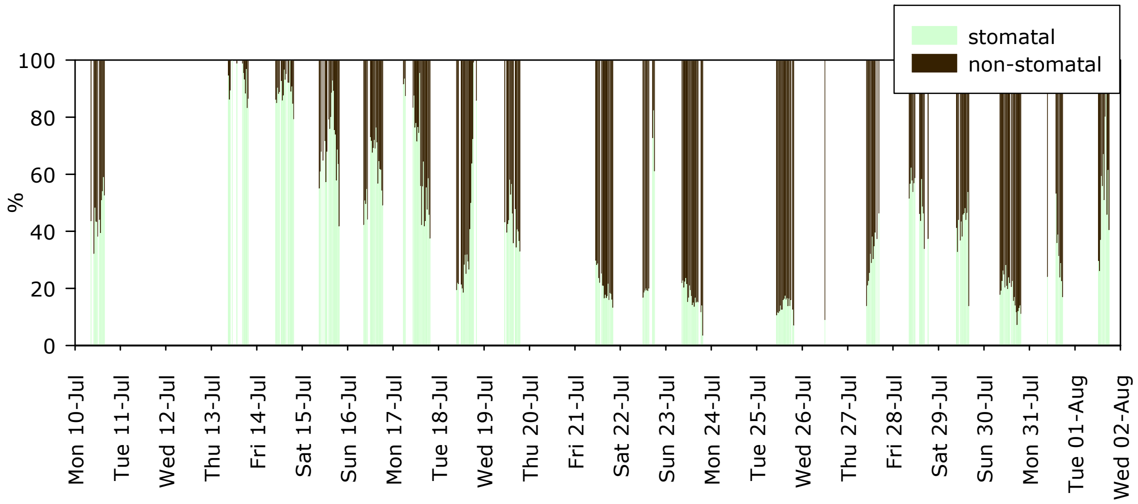

Figure 8 The percentage of the total flux that is either stomatal or non-stomatal.